RESEARCH ARTICLE

National Science Review
11: nwae016, 2024
https://doi.org/10.1093/nsr/nwae016
Advance access publication 11 January 2024

CHEMISTRY

Universal insertion of molecules in ionic compounds under pressure

Feng Peng[1,2], Yanming Ma[3,4], Chris J. Pickard[5,6], Hanyu Liu[3,4,*] and Maosheng Miao[2,7,*]

[1]College of Physics and Electronic Information, Luoyang Normal University, Luoyang 471022, China; [2]Department of Chemistry and Biochemistry, California State University Northridge, Northridge 91330, USA; [3]State Key Laboratory of Superhard Materials & Key Laboratory of Material Simulation Methods and Software of Ministry of Education, College of Physics, Jilin University, Changchun 130012, China; [4]International Center of Future Science, Jilin University, Changchun 130012, China; [5]Department of Materials Science & Metallurgy, University of Cambridge, Cambridge CB3 0FS, UK; [6]Advanced Institute for Materials Research, Tohoku University, Sendai 980-8577, Japan and [7]Department of Earth Science, University of California Santa Barbara, Santa Barbara 93106, USA

*Corresponding authors. E-mails: mmiao@csun.edu; hanyuliu@jlu.edu.cn

Received 18 November 2022; **Revised** 18 October 2023; **Accepted** 1 November 2023

ABSTRACT

Using first-principles calculations and crystal structure search methods, we found that many covalently bonded molecules such as H_2, N_2, CO_2, NH_3, H_2O and CH_4 may react with NaCl, a prototype ionic solid, and form stable compounds under pressure while retaining their molecular structure. These molecules, despite whether they are homonuclear or heteronuclear, polar or non-polar, small or large, do not show strong chemical interactions with surrounding Na and Cl ions. In contrast, the most stable molecule among all examples, N_2, is found to transform into cyclo-N_5^- anions while reacting with NaCl under high pressures. It provides a new route to synthesize pentazolates, which are promising green energy materials with high energy density. Our work demonstrates a unique and universal hybridization propensity of covalently bonded molecules and solid compounds under pressure. This surprising miscibility suggests possible mixing regions between the molecular and rock layers in the interiors of large planets.

Keywords: molecule-solid hybrid materials, high-pressure, crystal structure prediction, density functional theory, planet interior

INTRODUCTION

Chemical substances are generally divided into two large categories: molecules and solid-state compounds. They distinctly differ in structures, bonding features, and properties and have been used in different areas. Molecules are generally formed from nonmetals and are held together by covalent bonds, whereas solid-state compounds often comprise metals or metalloids and can be characterized by ionic or metallic bonding. Hybrid materials, which consist of inorganic components and small molecules, have gained intensive attention owing to their unique chemical structure, physical properties, and potential applications in optics, electronics, mechanics, catalysis, and sensors as well as biomedical devices [1–5]. However, these unique characteristics also impose challenges on material synthesis, characterization, as well as the fundamental understanding of their chemical behavior.

The formation of most hybrid materials usually is caused by strong chemical interactions between inorganic species, such as ions and atoms, and small organic molecules. For instance, well-known hydrate compounds can be considered as a class of hybrids in which water molecules (H_2O) are chemically integrated into inorganic crystal structures. Notably, $CuSO_4$ forms hydrates of the form $CuSO_4{\cdot}nH_2O$ where n can range from 1 to 7 [6]. In these compounds, the lone-pair electrons in H_2O form coordinate bonds with the d orbitals of transition metal hosts. NaCl, a classic ionic solid, can also form hydrates, especially under elevated pressure conditions. This phenomenon is driven by the screening of electrostatic potentials by highly polar molecules such as H_2O. This interaction mirrors the solvation of NaCl in polar solvents, whereby water molecules surround and isolate individual sodium and chloride ions.

One of the more recent and notable examples of hybrid materials is organic-inorganic hybrid perovskites. These materials have gained significant attention due to their promising efficiency as photovoltaic materials. The formation of these perovskites is largely attributed to the strong ionic interactions between the negatively charged inorganic anions and the positively charged organic cations. This hybrid structure offers a promising route toward the design of next-generation energy materials [7].

In the current investigation, we aim to explore a distinctive new category of hybrid materials whose formation is not facilitated by strong chemical interactions between molecules and the encompassing inorganic species. Our study was inspired by recent research into the unique chemistry that emerges under high pressure. Under these conditions, the chemical properties of elements and the strengths of the homonuclear and heteronuclear bonds can change drastically, leading to the formation of many atypical compounds with non-intuitive compositions and structures, like $NaCl_3$, Fe_3Xe, and CsF_3 [8–10].

Moreover, many recent theoretical and experimental studies have revealed that helium (He) can react with various ionic crystals to form stable ternary compounds under high pressure. In these compounds, He, despite being a noble gas, is integrated into the crystal structure without forming localized bonds with neighboring atoms. In this context, several pressure-stabilized He compounds have been predicted or synthesized, such as MgF_2He, FeO_2He, and Na_2He [11–13]. These observations signal an unprecedented capacity of He to interact with other substances under high-pressure conditions, despite its known chemical inertness.

In this study, we aim to expand upon this concept of helium insertion with a view to investigating the potential for inserting small molecules, e.g. H_2, N_2, CO_2, NH_3, H_2O, and CH_4 *et al.*, into ionic compounds under pressure. The examples are carefully chosen to represent homonuclear and heteronuclear molecules, non-polar and polar molecules, and molecules with different sizes. Unlike helium, which is highly resistant to forming chemical bonds, these small molecules generally have a much higher chemical reactivity. However, our comprehensive crystal structure search studies reveal a compelling general chemical trend under high-pressure conditions. Despite their higher chemical activity compared to helium, most of these small molecules surprisingly retain their integrity when inserted into prototypical ionic compounds, such as NaCl. This leads to the formation of thermodynamically stable hybrid compounds, opening up exciting new possibilities in exploring unconventional hybrid materials.

An immediate application of our study is the understanding of the composition and structure of planets' interiors. All large planets consist of both covalently bonded molecules and solid-state minerals, segregated into different layers with large dispersive regions. Mars and Venus consist of three layers: a rocky (iron-nickel/sulfide) core in the center, a silicate mantle in the middle and an outer composed mainly of gaseous carbon dioxide (CO_2) and nitrogen (N_2). The interiors of Uranus and Neptune are mainly composed of a rocky (silicate/iron-nickel) core in the center and icy mantle (water, ammonia, and methane, along with traces of other hydrocarbons, but not necessarily for these molecules). There are abundant ionic compounds and small molecules in the boundary of mantle-outer layer (Mars and Venus) and core-mantle (Uranus and Neptune) boundaries. Our investigations on structures and physical properties of salt-SM hybrid compounds will provide key information to the understanding of the interior structure and dynamics of these planets. Especially, minerals and SM both exist in a variety of ocean exoplanets' interiors, namely salty high-pressure ice (NaCl-H_2O) [14,15].

To this end, we performed extensive structure searches to examine the possibility of forming hybrid salt-SM materials under high pressure [16,17]. Our simulations uncovered a variety of stable NaCl-SM compounds with various compositions at a wide pressure range of up to 200 GPa. Among all predicted structures, $NaCl(H_2)_4$ and $NaCl(N_2)_5$ compounds could be stable at pressures of 38 and 36 GPa, respectively. Our current findings not only establish a new family of hybrid salt-SM compounds for further design and discovery of intriguing materials, especially for the combination of inorganic compounds and small organic molecules under high pressure, but also provide crucial implications for the understanding of the interior of exoplanets. In addition, NaCl is often employed as a pressure-transmitting medium and thermal insulator in diamond anvil cell experiments due to its high compressibility, low strength, and limited chemical reactivity as well as its general ease of use. The present results also provide useful suggestions on the effectivity and the chemical limit of a solid NaCl pressure-transmitting medium.

RESULTS AND DISCUSSION

First, we conducted an extensive exploration on the high-pressure phase diagrams of NaCl-SM (SM = H_2, N_2, CO_2, NH_3, H_2O, CH_4) hybrid compounds at high pressures by performing swarm-intelligence based CALYPSO [18,19] structure searches. The thermodynamic stability of NaCl-SM hybrid compounds is evaluated from their formation enthalpies relative to the dissociation products of NaCl + SM. In principle, NaCl-SMs are ternary compounds and may have a great amount of different possible decomposition products. However, all structure searches show that there is no sign of SM dissociation at the pressures considered in this study, which allows us to treat SM as a single reaction unit. On the other hand, NaCl has the most stable stoichiometry among all metal halides

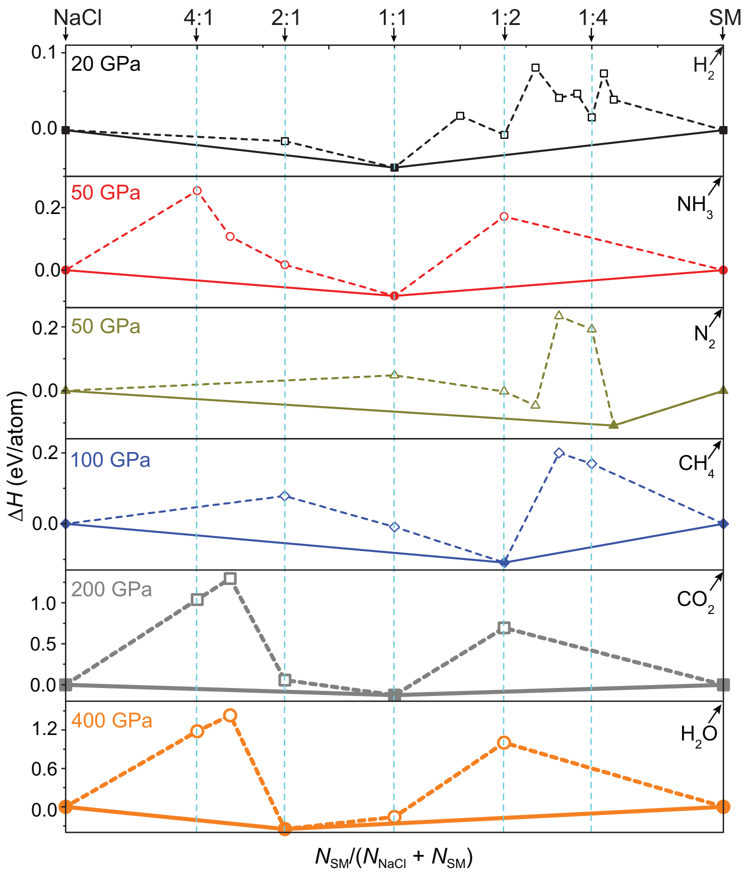

Figure 1. Phase stabilities of various NaCl-SM hybrid compounds. Enthalpies of formation of NaCl-SM (SM = H_2, N_2, CO_2, NH_3, H_2O, CH_4) under several pressures. Dotted lines connect the data points, and solid lines denote the convex hull.

at ambient conditions and the high-pressure range used in this study [20,21]. Therefore, we reduce the stability evaluation to a pseudo-binary reaction of $m\text{NaCl} + n\text{SM} \rightarrow m\text{NaCl}\ (\text{SM})_n$. For NaCl, the known body-centered cubic and face-centered cubic structures are considered in their corresponding stable pressure ranges. The phases of $P6_3/mc$, ε-N, I-$42d$, $P2_12_12$, $Pbcm$ and $Pnma$ are considered for H_2, N_2, CO_2, NH_3, H_2O, and CH_4 in their corresponding pressure, respectively. As a consequence, our simulations identified a series of hitherto unknown NaCl-SM (SM = H_2, N_2, CO_2, NH_3, H_2O, CH_4) hybrid compounds under high pressure, as shown in Fig. 1. In this work, we take hybrid $NaCl(H_2)_4$ compound as an example, since this structure is predicted to become thermodynamically stable at sub-megabar pressures of 38 GPa.

As shown in Fig. 1, at 20 GPa, $NaClH_2$ is the only stable composition, but at a higher pressure of 100 GPa, both $NaClH_2$ and $NaCl(H_2)_4$ (containing four H_2 molecules) (Fig. S1) become stable. As the pressure increases from 20 to 100 GPa, the formation enthalpy of $NaClH_2$ increases from −49 meV/atom to −192 meV/atom. These results indicate that pressure could significantly promote the formation of stable salt-H_2 compounds with a higher H_2 content. Besides, we also attempted to study other hybrid salt-H_2 stabilities under high pressure, such as KI-H_2, RbI-H_2 and RbBr-H_2 (Fig. S1). The stable pressure range of the hybrid salt-H_2 compounds are summarized in Fig. S1d. It is remarkable that KI forms a hybrid compound with H_2 at the lowest pressure of 1 GPa, and therefore the possibility of future experimentation is greatly stimulated. It is noted that the $NaClH_x$ compounds have been recently synthesized [22], in which our predicted $NaClH_2$ with $P6_3/mmc$ symmetry [23] agrees well with the structure observed in the experiment (Table S2 and Fig. S13). This greatly encourages us to study other NaCl-SM hybrid compounds, although our predicted $NaCl(H_2)_4$ with Pm symmetry was not observed. We found that the hybrid salt-H_2 compounds become less stable with increasing cation radius from NaCl to CsCl. In contrast to the trend of the cation, the increased size of the anion increases the stability of the hybrid salt-H_2 compounds. These results indicate that the difference in the sizes of the cation and the anion is a determining factor in the formation of stable hybrid compounds with H_2 molecules, which naturally explains the reason for the ultra-low-pressure threshold of KI-H_2 (Fig. S1c). This offers an unexpected prospect for the storage of hydrogen in the salt, and other similar ionic compounds.

The above calculations fully include the effects of van der Waals (vdW) interactions and zero-point energies (ZPE), which may play critical roles in determining the stability of these predicted hydrogen-rich compounds. After considering these effects, the formation energies of the hybrid salt-H_2 compounds remain almost unchanged, while transition pressures of these compounds are slightly different from those without considering these effects. For example, the phase transition pressure for the Pc to $P6_3/mmc$ structures is 14.6 GPa as compared to the static lattice PBE result of 16.5 GPa for $NaClH_2$ (Fig. S27), and the formation pressures of $NaClH_2$ are 15.3 and 17.4 GPa with and without vdW interactions, respectively. Once the ZPE is included, however, the formation pressure for $NaClH_2$ becomes 19.7 GPa.

Our structure searches reveal unique, and in many cases surprisingly simple, structural features for the salt-SM hybrid compounds. Depending on the concentration of H_2, our predicted structures represent three different ways of inserting H_2 molecules into the lattices of the salt: at atomic sites (Fig. 2a, $NaClH_2$ with $P6_3/mmc$ symmetry), inside tubes (Fig. 2b, $NaI(H_2)_2$ with $P2_12_12_1$ symmetry), and between layers (Fig. 2c, $NaBr(H_2)_2$ with $Pmmn$ symmetry) with increasing hydrogen content. In

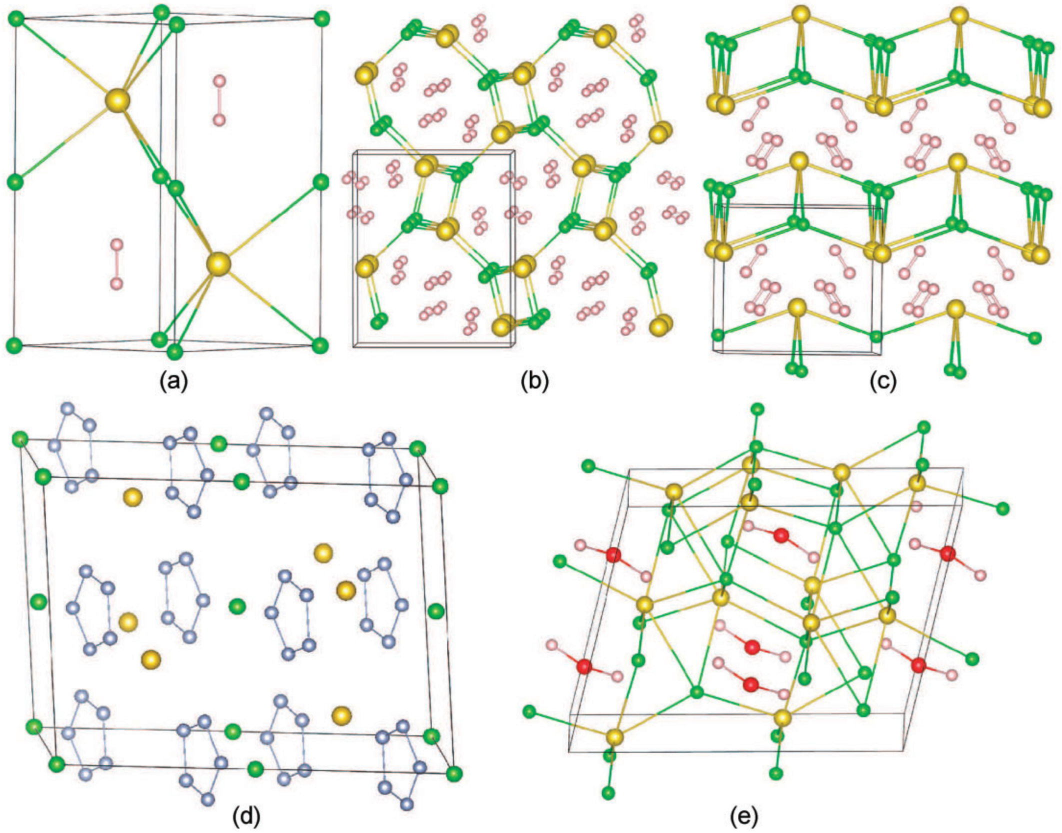

Figure 2. Structures of salt-SM hybrid compounds. Three different ways of inserting SM molecules inside the lattices of the NaCl: at atomic sites in $NaClH_2$ with $P6_3/mmc$ symmetry at 20 GPa (a); inside tubes in $NaI(H_2)_2$ with $P2_12_12_1$ symmetry at 50 GPa (b); and between layers in $NaBr(H_2)_2$ with $Pmmn$ symmetry at 30 GPa (c). (d) $NaClN_{10}$ with $C2/c$ symmetry at 50 GPa; (e) $(NaCl)_2H_2O$ with $C2/c$ symmetry at 300 GPa. The red, pink, grey, gold and green spheres represent O, H, N, Na and Cl atoms, respectively.

addition to the study on thermodynamic stability of these predicted structures, we have also investigated their dynamic stability, and the results indicate most of them are found to be recoverable when the pressure is partially or completely released. For example, the phonon calculations reveal no imaginary vibrational modes for the $NaClH_2$ in Pc phase (Fig. S37a), KIH_2 in the $P6_3/mmc$ structure (Fig. S14a), and $RbI(H_2)_2$ in the $Pmmn$ structure (Fig. S14c) at ambient conditions.

We will investigate the chemical interaction between SM and the ionic sublattices by various electronic structure analysis methods, including a rigid band structure analysis, Bader's quantum theory of atoms in molecules (QTAIM) [24], electron localization functions (ELFs) [25], projected density of states (PDOS), and crystal orbital hamilton population (COHP) [26]. Our study will focus on NaCl-H_2 compounds. The bonding features in all salt-SM compounds are quite similar.

The band structure of $NaClH_2$ at ambient pressure shows a large energy band gap of nearly 5.6 eV (Fig. 3a). This value is close to the NaCl band gap under ambient pressure. In order to verify the effect of electroneutral H_2 insertion on the electronic structure of the ionic sublattice, we also constructed a model system of $NaClH_0$, in which all the H_2 molecules are removed from the system. By comparing the band structures of $NaClH_2$ with $NaClH_0$, as shown in Fig. 3a, the results show that the H_2 molecules do not significantly interfere with NaCl bands around the Fermi energy, which also suggests weak interactions between the H_2 molecule and the ionic sublattice. Two groups of valence bands are heavily involved in H_2 insertion in $NaClH_2$, the upper one ranges from the Fermi level (0 eV) to −2.5 eV, and the lower one ranges from about −4.9 eV to −7.1 eV. After checking the projected components, we found that the upper groups are mainly the Cl *3p* orbitals, whereas the lower group are mainly the H *1s* orbitals. The bands in the upper group correspond to the Cl *3p* bands in $NaClH_0$ (dashed red lines). The insertion of H_2 into the NaCl lattice alters these bands to a considerable amount due to the occupation of the interstitial sites surrounded by Cl^- ions. On the other hand,

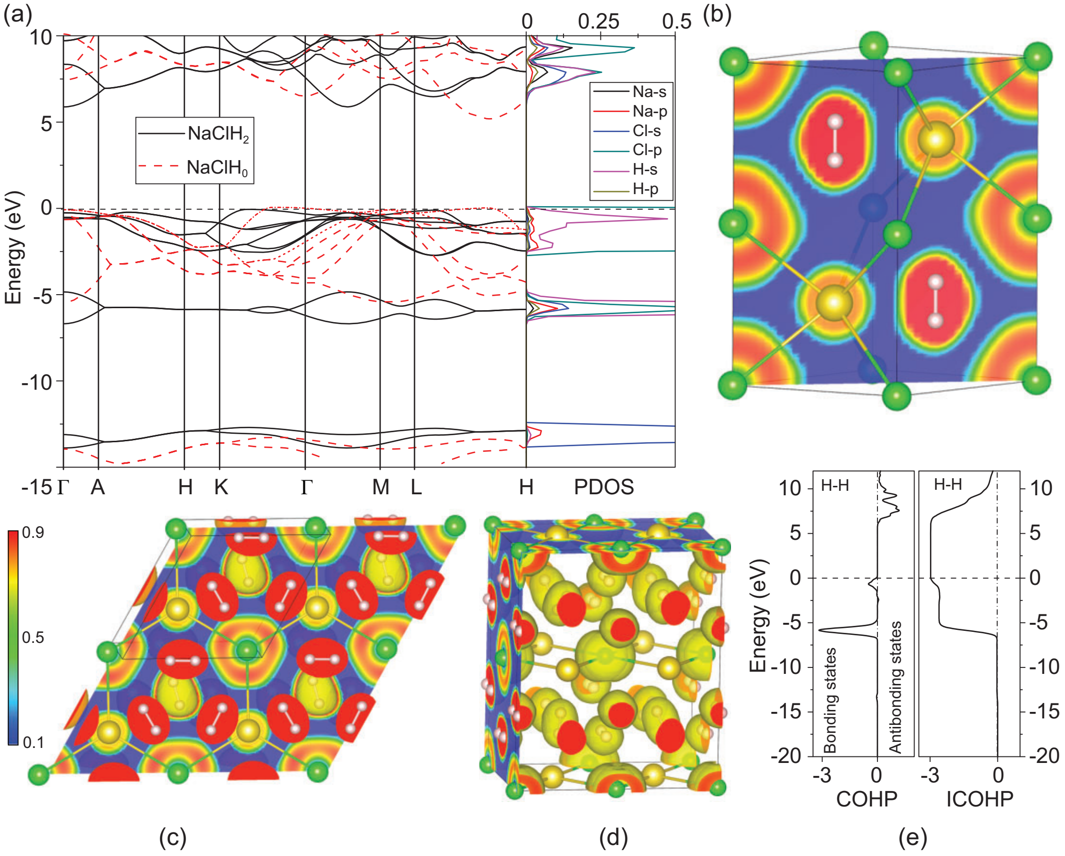

Figure 3. Calculated electronic properties for NaClH$_n$ at various pressures. (a) The electronic band structure and PDOS of *P*6$_3$/*mmc* phase for NaClH$_2$ at 20 GPa. In the left panel, the black solid lines are the electronic band structure of NaClH$_2$; the red dashed lines are those of NaClH$_0$ in which all the H$_2$ molecules are removed from the NaClH$_2$ structure. The black and red dashed lines show the Fermi energies of NaClH$_2$ and NaClH$_0$. The right panel presents the projected DOS of NaClH$_2$. (b–d) The calculated ELFs of NaClH$_2$ with *P*6$_3$/*mmc* phase at 20 GPa, NaCl(H$_2$)$_4$ with *Pm* symmetry at 50 GPa, and NaCl(H$_2$)$_4$ with *Cmmm* symmetry at 100 GPa. (e) Calculated COHP and ICOHP of NaClH$_2$ at 20 GPa.

the H$_2$ bands only slightly overlap with Cl$^-$ and Na$^+$ states, indicating a weak interaction. This feature will be further proved by the following ELF and COHP calculations. Interestingly, the similar band structure and PDOS in all the salt-(H$_2$)$_n$ and other NaCl(SM)$_n$ systems (Figs S18–S29) confirmed the weak interaction between NaCl and SM, implying the insertion nature of molecules in ionic compounds.

The Bader QTAIM charge [24] calculations (Table S1) support a model of NaCl ionic compounds inserted by neutral H$_2$ molecules. The Bader charges on Na, Cl, and H atoms are found to be 0.88, −0.85, and 0.33 under 0 GPa, respectively. It is typical that the Bader charges are significantly smaller than the nominal charges. For example, the Bader charges of Na and Cl in NaCl crystal under 0 GPa are 0.82 and −0.82. For the same reason, the small residual charges found on H do not indicate the charge transfer between H$_2$ and NaCl lattices. As a matter of fact, the insertions of He into NaCl and elemental Na also show a small charge of 0.83 under 50 GPa and of 0.81 under 100 GPa.

In conjunction with the Bader charge results, the ELF [25] calculations (Fig. 3b–d) reveal that inserted H$_2$ molecules do not strongly bond with surrounding Na$^+$ and Cl$^-$ ions. The ELFs of *Pm* phase at 50 GPa (Fig. 3c) and *Cmmm* phases for NaCl(H$_2$)$_4$ at 100 GPa (Fig. 3d) unambiguously show the same bonding nature of Na–Cl and H–H. The low ELF values between Na and Cl confirm the ionic bonding nature (Fig. 3b), whereas the high ELF values between neighboring H atoms are in accordance with the fact that neighboring H atoms are covalently bonded and form H$_2$ molecules. On the other hand, the low ELF values reveal very weak local bonding between H$_2$ molecular units and the surrounding ions in both compounds. Similar results are found for other salt-SM hybrid compounds predicted in this work.

To further examine the bonding strength, we calculated the COHPs [26] and the integrated COHPs

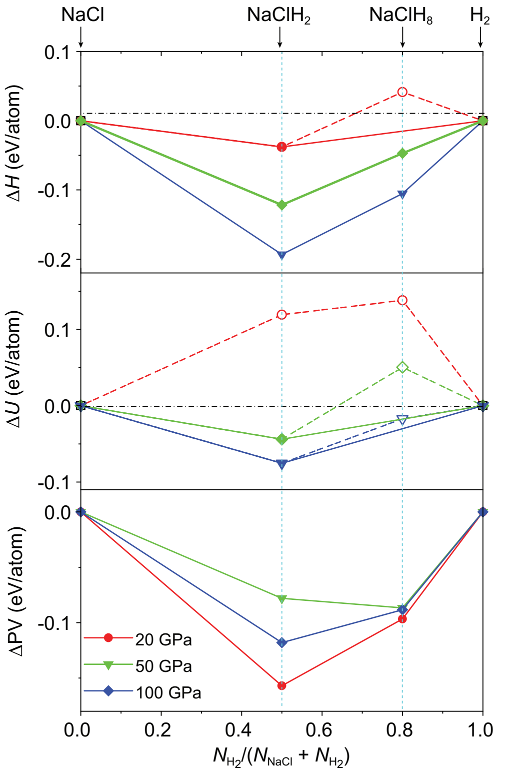

Figure 4. Energy contributions to the formation of NaCl-H_2 hybrid compounds. Reaction enthalpies (top panel), internal energy changes (middle panel), and PV term changes (bottom panel) for the formation of NaCl-H_2 hybrid compounds at different pressures.

(ICOHP) between neighboring atoms in these compounds. The results show the full occupation of the H–H bonding states and the empty H–H antibonding states, revealing that the bonding feature of H_2 molecules is not largely influenced while inserted into the NaCl crystal (Fig. 3e). For comparison, we calculated the ICOHP values up to the Fermi level for H–H pairs in NaCl-H_2 compounds and in solid hydrogen at various pressures. The ICOHP value of −2.9 pairs/eV of the H–H bond reveals the strength of H–H in salt-H_2 systems. This is also in conformity with the fact that the bond length (0.72 Å) of H_2 in salt-H_2 is close to that (0.74 Å) in pure solid H_2.

If the inserted molecules do not interact strongly with the surrounding ions, what mechanism drives the formation of these unusual hybrid compounds under pressure? We thoroughly investigate the origin of the thermodynamic stability of the salt-SM compounds, starting from the split of the reaction enthalpies of NaCl-H_2 compounds as shown in Fig. 4, ΔH, into the internal energy changes ΔU and the pressure-volume terms ΔPV.

For $NaClH_2$, although ΔU is positive at low pressure whereas ΔPV is negative, both terms decrease with increasing pressure, contributing to the continuous decrease of ΔH, leading therefore to the stabilization of the hybrid compound. In particular, the ΔPV term decreases much more significantly than ΔU, indicating that the formation of XY-H_2 hybrid compounds is primarily driven by volume reduction. For compounds with higher hydrogen composition, such as $NaCl(H_2)_4$, the decrease in ΔPV is less significant. However, it still makes major contributions to the reaction enthalpy and the stabilization of inserted compounds. It is worth noting that many recently predicted and synthesized metal hydrides, such as NaH_n [27], LiH_n [28] *etc*, contain H_2 molecules in their crystal lattices. Many of these hydrides can be viewed as XH-H_2 hybrid compounds, further demonstrating that the small molecule inclusion is an extensive phenomenon under high pressure.

Most other molecules, such as H_2O, NH_3, CH_4, and CO_2, behave similarly to H_2 while inserted into NaCl, i.e. they do not bond strongly with the neighboring Na^+ and Cl^- ions. In contrast, while searching low enthalpy structures of N_2-inserted NaCl, we found a striking phenomenon, namely, N_2 molecules will decompose in NaCl and form pentazolate anions (cyclo-N_5^-) (Fig. 2d) inserted into the NaCl crystal at pressures ranging from 36 to 83 GPa (Fig. S16a). Calculated ICOHP values for the N–N bond at 50 GPa is −1.56 eV/pair, indicating that there is a strong covalent bond of N–N in cyclo-N_5^- units (Fig. S16c). The Bader QTAIM calculations show charges of 0.86, 0.28, and −0.114 for Na, Cl, and N atoms, which suggest a large charge transfer from Cl^- to cyclo-N_5^-. Therefore, the formation of $NaCl(N_5)_2$ is due to the oxidation of Cl^- by cyclo-N_5^-. The band structure and PDOS of $C2/c$-$NaCl(N_5)_2$ at 50 GPa (Fig. S16b) show that the electron states of the cyclo-N_5^- contribute to both valence and conduction bands in a large energy range around the Fermi level and overlap with states of Na and Cl. Pentazolates are promising candidates for high-energy-density materials that do not release harmful products upon decomposition. However, its syntheses are hindered by low stability and usually involve additions of metal and organic stabilizers, forming complex structures. Our research shows that the commonly known ionic compounds such as NaCl that are easy to obtain and handle can be used to react directly with N_2 under pressure and produce compounds containing large compositions of pentazolate anions. As a matter of fact, the predicted $NaCl(N_5)_2$ structure has nearly 71% weight ratio of nitrogen in the form of cyclic N_5 units. The ambient-pressure decomposition of $NaCl(N_5)_2$ is estimated to possibly release 3.78 $kJ \cdot g^{-1}$ energy per $NaCl(N_5)_2$ unit. Moreover, our molecular dynamics simulations confirm the metastable feature of this predicted structure at ambient conditions (Fig. S17). The present results may open a new avenue to discover high-energy-density materials of polynitrogen compounds.

Although the crystal structure search predicts that H_2O molecules insert in NaCl similarly to H_2, the potentially stronger interactions between the H_2O molecule and surrounding ions merit an in-depth analysis of its electronic structure. As shown in Fig. 1 and Fig. S16d, the predicted monoclinic structure of $(NaCl)_2H_2O$ with *Pnma* symmetry (Fig. 2e) can become stable at a high pressure of 102 GPa. Furthermore, the band structure and PDOS for the $C2/c$ structure at 200 GPa (Fig. S16e) show that the entire energy range is dominated by the bands of the Cl anion. A large band gap of nearly 4.2 eV appears between the valence and conduction bands. The calculated COHP (Fig. S16f) clearly shows that the O–H bonding states are occupied, whereas the antibonding states are not. Correspondingly, the ICOHP value with −1.0 eV/pair of O–H bonds supports the strong covalent nature of O–H covalent bonding in H_2O molecules. Despite the stronger interactions with the surrounding ions, H_2O maintains its major molecular bonding features while inserted into NaCl.

Our results provide an important piece of knowledge for the understanding of the interior structure and dynamics of planets. Uranus and Neptune are called ‘ice giants’ in our solar system because they contain significant amounts of icy materials (mainly H_2O, CH_4, and NH_3). In addition, abundant ionic compounds exist in the rocky layer of Mars, Venus, Uranus, and Neptune. It is widely accepted that most exoplanets may assume similar multi-shell structures consisting of layers of molecular and ionic rocky materials. Thus, the molecule–rock interaction and its properties under pressure may govern the interlayer structures of most intermediate-mass exoplanets. While our study demonstrates that typical ionic compounds such as NaCl can react with icy materials, the general chemistry it reveals can potentially be extended to other compounds, including the rock materials, such as binary and ternary oxides, in the planet’s interior. Indeed, recent works uncovered that magnesium oxide–water compounds could become stable at high pressure and offered a renewed understanding of planetary interiors [29].

CONCLUSIONS

In conclusion, we demonstrate a unique chemical phenomenon under pressure using the first-principles calculations and the crystal structure search method: many covalently bonded molecules can form stable compounds by mixing into ionic crystals while maintaining their molecular integrity. The phenomenon is manifested in many striking predictions. For example, H_2 is predicted to react with NaCl to form $NaClH_2$ and $NaCl(H_2)_4$ at 20 and 38 GPa pressures, respectively. A similar reaction could happen at a much lower pressure of 1 GPa if H_2 is inserted into potassium iodide (KI), which facilitates future experimental synthesis and applications by bringing the reaction pressure down to the sub-GPa level. Similar insertions are also found for heteronuclear molecules such as H_2O, NH_3, and CH_4, despite whether the molecule is polar or nonpolar. The crystal structure search also predicted the insertion of C_2H_6 into NaCl under high pressure, indicating the wide range of the phenomenon and the possibility that large organic molecules might be chemically reserved inside the rocky interior of planets. Last, to our surprise, the most stable one among all molecules in this work, $N_{2,}$ is found to transform chemically while inserted into NaCl and become cyclo-N_5^- which oxidizes NaCl. This reaction could become a new route to synthesize and stabilize pentazolates, green energy materials with high energy density. Our results suggest that the molecular and rock layers in the interiors of large planets may exhibit large regions in which the molecules and solid compounds diffuse into each other and are chemically mixed.

METHODS

Crystal structure prediction

Our structure searching simulations are performed through the swarm-intelligence based CALYPSO method [18] via a global minimization of free energy surfaces merging *ab initio* total-energy calculations as implemented in the CALYPSO code [19] and random structure searching as implemented in the AIRSS code [30,31]. These methods are specially designed for unbiased global structural optimization, and have been benchmarked on various known systems [31–34].

Total energy calculations

Total energy calculations were performed in the framework of density functional theory within the Perdew-Burke-Ernzerhof [35] parameterization of generalized gradient approximation [36] as implemented in the VASP (Vienna Ab Initio simulation package) code [37]. The projector-augmented wave (PAW) method [38] was adopted with the PAW potentials taken from the VASP library where *d* electrons are treated as valence electrons for alkali elements. The use of the plane-wave kinetic energy cutoff of 1200 eV (for H_2 molecules) and 800 eV (for NH_3, H_2O, CH_4, CO_2, N_2 molecules) and dense k-point sampling, adopted here, were shown to give excellent convergence of total energies (within ∼1 meV/atom). We explored the zero-point energy effects on the formation energy using the phonopy code [39].

SUPPLEMENTARY DATA

Supplementary data are available at *NSR* online.

FUNDING

M.M. acknowledges the support of National Science Foundation (NSF) funds DMR 1848141 and OAC 2117956, ACF PRF 59249-UNI6, and the Camille and Henry Dreyfus Foundation. F.P. and Y.M. acknowledge funding support from the National Natural Science Foundation of China (12174170 and 11774140), Program for Innovative Research Team (in Science and Technology) in University of Henan Province (24IRTSTHN026) and Excellent Youth Foundation of Henan Scientific Committee (232300421020). C.J.P. acknowledges financial support from the Engineering and Physical Sciences Research Council (EPSRC) of the UK (EP/P022596/1) and also acknowledges financial support from the Royal Society through a Royal Society Wolfson Research Merit award.

AUTHOR CONTRIBUTIONS

M.M. and H.L. designed the research; F.P. performed the calculations; all authors analyzed and interpreted the data, and contributed to the writing of the paper.

Conflict of interest statement. C.J.P. is an author of the CASTEP code and receives royalties on its commercial sales by Dassault Systemes.

REFERENCES

1. Sanchez C, Shea KJ, Kitagawa S. Recent progress in hybrid materials science. *Chem Soc Rev* 2011; **40**: 471–2.
2. Dresselhaus MS and Thomas IL. Alternative energy technologies. *Nature* 2001; **414**: 332–7.
3. Yang J, Sudik A, Wolverton C *et al.* High capacity hydrogen storage materials: attributes for automotive applications and techniques for materials discovery. *Chem Soc Rev* 2010; **39**: 656–75.
4. Rosi NL, Eckert J, Eddaoudi M *et al.* Hydrogen storage in microporous metal-organic frameworks. *Science* 2003; **300**: 1127–9.
5. Yang Y, Ji J, Feng J *et al.* Two-dimensional organic–inorganic room-temperature multiferroics. *J Am Chem Soc* 2022; **144**: 14907–14.
6. Singh M, Kumar D, Thomas J *et al.* Crystallization of copper(II) sulfate based minerals and MOF from solution: chemical insights into the supramolecular interactions. *J Chem Sci* 2010; **122**: 757–69.
7. Gao ZS, An H, Lv L *et al.* Study on CH_4 adsorption onto the surfaces of perovskite ABO_3 (A=La, Ba; B=Zr, Co, Ce) by density functional theory. *Adv Mater* 2011; **291**: 1208–11.
8. Zhang W, Oganov AR, Goncharov AF *et al.* Unexpected stable stoichiometries of sodium chlorides. *Science* 2013; **342**: 1502–5.
9. Zhu L, Liu H, Pickard CJ *et al.* Reactions of xenon with iron and nickel are predicted in the Earth's inner core. *Nat Chem* 2014; **6**: 644–8.
10. Miao M. Caesium in high oxidation states and as a *p*-block element. *Nat Chem* 2013; **5**: 846–52.
11. Liu Z, Botana J, Hermann A *et al.* Reactivity of He with ionic compounds under high pressure. *Nat Commun* 2018; **9**: 951.
12. Zhang J, Lv J, Li H *et al.* Rare helium-bearing compound FeO_2He stabilized at deep-earth conditions. *Phys Rev Lett* 2018; **121**: 255703.
13. Dong X, Oganov AR, Goncharov AF *et al.* A stable compound of helium and sodium at high pressure. *Nat Chem* 2017; **9**: 440–5.
14. Klotz S, Bove LE, Strässle T *et al.* The preparation and structure of salty ice VII under pressure. *Nat Mater* 2009; **8**: 405–9.
15. Hernandez JA, Caracas R, Labrosse S. Stability of high-temperature salty ice suggests electrolyte permeability in water-rich exoplanet icy mantles. *Nat Commun* 2022; **13**: 3303.
16. Zhang L, Wang Y, Lv J *et al.* Materials discovery at high pressures. *Nat Rev Mater* 2017; **2**: 17013.
17. Oganov AR, Pickard CJ, Zhu Q *et al.* Structure prediction drives materials discovery. *Nat Rev Mater* 2019; **4**: 331–48.
18. Wang Y, Lv J, Zhu L *et al.* Crystal structure prediction via particle-swarm optimization. *Phys Rev B* 2010; **82**: 094116.
19. Wang Y, Lv J, Zhu L *et al.* CALYPSO: a method for crystal structure prediction. *Comput Phys Commun* 2012; **183**: 2063–70.
20. Sata N, Shen G, Rivers ML *et al.* Pressure-volume equation of state of the high-pressure B_2 phase of NaCl. *Phy Rev B* 2002; **65**: 104114.
21. Sakai T, Ohtani E, Hirao N *et al.* Equation of state of the NaCl-B_2 phase up to 304 GPa. *J Appl Phys* 2011; **109**: 084912.
22. Matsuoka T, Muraoka S, Ishikawa T *et al.* Hydrogen-storing salt $NaCl(H_2)$ synthesized at high pressure and high temperature. *J Phys Chem C* 2019; **123**: 25074–80.
23. Peng F, Ma Y, Miao M. High-pressure hybrid materials that can store hydrogen in table salt. ArXiv: 1907.08295v1.
24. Bader RFW. Atoms in molecules. *Acc Chem Res* 1985; **18**: 9–15.
25. Silvi B and Savin A. Classification of chemical bonds based on topological analysis of electron localization functions. *Nature* 1994; **371**: 683–6.
26. Deringer VL, Tchougréeff AL, Dronskowski R. Crystal orbital Hamilton population (COHP) analysis as projected from plane-wave basis sets. *J Phys Chem A* 2011; **115**: 5461–6.
27. Baettig P and Zurek E. Pressure-stabilized sodium polyhydrides: NaH(n) (n>1). *Phys Rev Lett* 2011; **106**: 237002.
28. Zurek E, Hoffmann R, Ashcroft NW *et al.* A little bit of lithium does a lot for hydrogen. *Proc Natl Acad Sci USA* 2009; **106**: 17640–3.
29. Pan S, Huang T, Vazan A *et al.* Magnesium oxide-water compounds at megabar pressure and implications on planetary interiors. *Nat Commun* 2023; **14**: 1165.

30. Pickard CJ and Needs RJ. *Ab initio* random structure searching. *J Phys Condens Matter* 2011; **23**: 053201.
31. Pickard CJ and Needs RJ. High-pressure phases of silane. *Phys Rev Lett* 2006; **97**: 045504.
32. Peng F, Sun Y, Pickard CJ *et al.* Hydrogen clathrate structures in rare earth hydrides at high pressures: possible route to room-temperature superconductivity. *Phys Rev Lett* 2017; **119**: 107001.
33. Pickard CJ and Needs RJ. Structure of phase III of solid hydrogen. *Nat Phys* 2007; **3**: 473–6.
34. Pickard CJ and Needs RJ. Highly compressed ammonia forms an ionic crystal. *Nat Mater* 2008; **7**: 775–9.
35. Perdew JP and Wang Y. Accurate and simple analytic representation of the electron-gas correlation energy. *Phys Rev B* 1992; **45**: 13244–9.
36. Perdew JP, Burke K, Ernzerhof M. Generalized gradient approximation made simple. *Phys Rev Lett* 1996; **77**: 3865–8.
37. Kresse G and Furthmüller J. Efficient iterative schemes for *ab initio* total-energy calculations using a plane-wave basis set. *Phys Rev B* 1996; **54**: 11169–86.
38. Blöchl PE. Projector augmented-wave method. *Phys Rev B* 1994; **50**: 17953–79.
39. Togo A, Oba F, Tanaka I. First-principles calculations of the ferroelastic transition between rutile-type and $CaCl_2$-type SiO_2 at high pressures. *Phys Rev B* 2008; **78**: 134106.
